arXiv:physics/0512201v1 [physics.atom-ph] 21 Dec 2005

Hyperpolarizability effects in a Sr optical lattice clock

Anders Brusch, Rodolphe le Targat, Xavier Baillard, Mathilde Fouché, and Pierre Lemonde*
LNE-SYRTE, Observatoire de Paris
61, Avenue de l'Observatoire, 75014, Paris, France
(Dated: February 2, 2008)

We report the observation of the higher order frequency shift due to the trapping field in a ^{87}Sr optical lattice clock. We show that at the magic wavelength of the lattice, where the first order term cancels, the higher order shift will not constitute a limitation to the fractional accuracy of the clock at a level of 10^{-18}. This result is achieved by operating the clock at very high trapping intensity up to 400 kW/cm^2 and by a specific study of the effect of the two two-photon transitions near the magic wavelength.

PACS numbers: 06.30.Ft,32.80.-t,42.50.Hz,42.62.Fi

The recent proposal and preliminary realizations of optical lattice clocks open a promising route towards frequency standards with a fractional accuracy better than 10^{-17} [1, 2, 3, 4]. A large number of atoms are confined in micro-traps formed by the interference pattern of laser beams which in principle allows both the high signal to noise ratio of optical clocks with neutral atoms [5] and the cancellation of motional effects of trapped ion devices [6, 7, 8, 9]. In contrast to the ion case an optical lattice clock requires high trapping fields. The evaluation of their effects on the clock transition is a major concern and is the subject of this letter. For a Sr optical lattice clock, the typical requirement in terms of trapping depth is about $10\,E_r$ with E_r the recoil energy associated to the absorption of a lattice photon [10]. The corresponding frequency shift of both clock states amounts to 36 kHz at 800 nm, while a relative accuracy goal of 10^{-18} implies a control of the differential shift at the 0.5 mHz level, or 10^{-8} in fractional units.

The frequency of the clock transition in a laser trap of depth U_0 is shifted with respect to the unperturbed frequency ν_0 according to

$$\nu = \nu_0 + \nu_1 \frac{U_0}{E_r} + \nu_2 \frac{U_0^2}{E_r^2} + O\left(\frac{U_0^3}{E_r^3}\right), \qquad (1)$$

with ν_1 and ν_2 proportional to the (dynamic) polarizability and hyperpolarizability difference between both states of the clock transition [1]. By principle of the optical lattice clock, ν_1 cancels when the laser which forms the lattice is tuned to the "magic wavelength" λ_m. Although this remains to be demonstrated experimentally, a control of this first order term to better than 1 mHz seems achievable [1].

The higher order term is a priori more problematic with no expected cancellation. A theoretical calculation of the effect is reported in Ref. [1] predicting a frequency shift of $-2\,\mu\text{Hz}/E_r^2$ for a linear polarization of the lattice. The calculation however was performed at the theoretical magic wavelength of 800 nm. The actual value [17], $\lambda_m = 813.428(1)$ nm (see [2, 3] and below), lies near two two-photon resonances which may considerably enhance the effect and impede the realization of an accurate clock. The first one couples $5s5p\,^3P_0$ to $5s7p\,^1P_1$ (Fig. 1) and is at a wavelength of 813.36 nm, or equivalently 30 GHz away from the magic wavelength. Although this $J = 0 \to J = 1$ two-photon transition is forbidden to leading order for two photons of identical frequencies [11], it is so close to the magic wavelength that it has to be a priori considered. The second one resonantly couples $5s5p\,^3P_0$ to $5s4f\,^3F_2$ at 818.57 nm and is fully allowed.

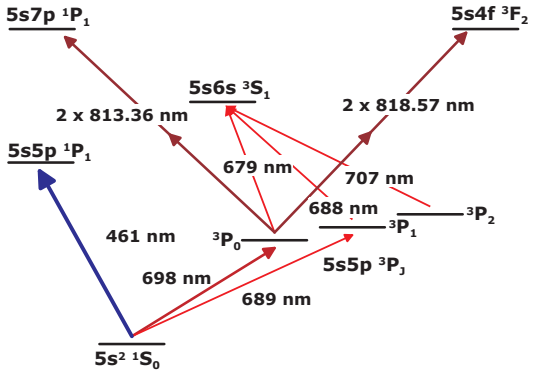

FIG. 1: Energy levels of Sr relevant to this paper. The clock transition at 698 nm couples the two lowest energy states of the atom.

We report here an experimental study of higher order effects in a ^{87}Sr optical lattice clock operating at a very high trapping depth up to $1400\,E_r$ and for a linear polarization of the lattice. This depth is about a factor of ten higher than in the other reported systems [2, 3] which enhances the sensitivity to higher-order frequency shifts by two orders of magnitude. At the maximum depth and for a detuning of the lattice laser as small as 0.5 GHz from the $^3P_0 \to {}^1P_1$ transition, higher order frequency shifts are below a few hertz. On the other hand, when the lattice laser is tuned to within a few hundred MHz of the $^3P_0 \to {}^3F_2$ transition, non-linear frequency shifts of several kHz are observed. These results, together with measurements at the magic wavelength, give a stringent limit

in optimal operating conditions. We show that higher order frequency shifts will not limit the accuracy of a Sr optical lattice clock down to the 10^{-18} level.

The high trapping depth is reached thanks to an enhancement Fabry-Pérot cavity around the 1D vertical lattice. The circulating power reaches 16 W for a 650 mW input at 813 nm. The mode has a waist radius of 90 μm corresponding to a maximum $U_0 = 1400\,E_r$ and an axial (resp. radial) oscillation frequency of 260 kHz (resp. 540 Hz). An intracavity dichroic mirror separates the lattice light from that which probes the clock transition. It induces negligible intracavity loss at 813 nm while ensuring that less than 10^{-3} of the incident power at 698 nm is reflected back to the atoms by the cavity mirror. The lattice polarization is interferometrically filtered by an intra-cavity quarter wave plate which lifts the degeneracy between the linear polarization states parallel to the eigen axis of the plate by half a free spectral range. The resulting polarization of the trapping light is linear to better than 10^{-3}. Its wavelength λ_L is controlled by means of a wave meter with an accuracy of 10^{-3} nm.

Atoms are loaded into the optical lattice from the magneto-optical trap (MOT) described in [12]. Throughout the loading cycle the lattice is overlapped with the MOT. Cold atoms at the center of the trap are selectively optically pumped to the metastable $^3P_{0,2}$ states by means of two "drain" lasers of waist radius 50 μm that are aligned to the lattice. They are tuned to the $^1S_0 - {}^3P_1$ and $^3P_1 - {}^3S_1$ transitions at 689 and 688 nm respectively (Fig. 1). Atoms in the metastable states remain trapped provided their energy is smaller than the 200 μK lattice depth. This leads to a continuous loading of the lattice at a rate of about 10^5 atoms/s. After half a second of loading time the MOT and drain lasers are switched off, and the atoms are repumped back to the ground state using two lasers tuned to the $^3P_{0,2} - {}^3S_1$ transitions at 679 and 707 nm. They are then cooled in the lattice to $\sim$ 10 μK in 50 ms with the narrow $^1S_0 - {}^3P_1$ intercombination line at 689 nm [13].

Following this preparation stage we probe the $^1S_0 - {}^3P_0$ clock transition at 698 nm. The frequency of the probe laser is referenced to an ultra-stable cavity as described in Ref. [14]. The probe beam is aligned parallel to the lattice and has a waist radius of 200 μm. Its polarization is linear and parallel to the lattice polarization. After the probe pulse, the transition probability to $^3P_0$ is measured in a few ms by laser induced fluorescence. A first detection pulse at 461 nm gives the number of atoms remaining in the ground state and ejects these atoms from the trap. Atoms in $^3P_0$ are then repumped to the ground state and detected similarly. This method allows a transition probability measurement which is insensitive to the atom number fluctuations. The resonance is shown in Fig. 2. The central feature (the carrier) is zoomed in the inset of the figure. Its linewidth is 260 Hz in optimal operating conditions: $\lambda_L = \lambda_m$, probe pulse of 10 ms duration and 2 μW power. The resonance plotted here was obtained at the maximum trapping depth and we observed no clear dependence of its width and contrast with U_0.

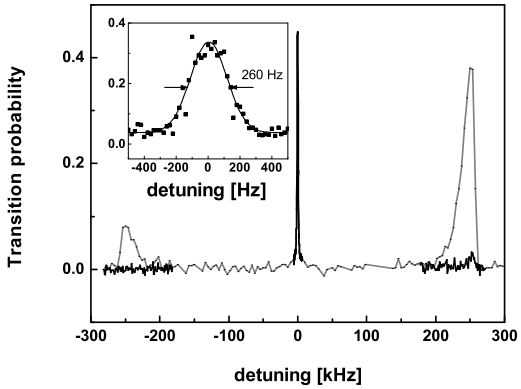

FIG. 2: Motional spectrum of the atoms in the optical lattice. Each point corresponds to a single measurement. Black curve: optimal operating conditions. The inset is a zoom on the carrier. Grey curve: the motional sidebands are enhanced by applying long probe pulses of 200 ms at the maximum available power at 698 nm.

The carrier is surrounded by motional sidebands shifted by the oscillation frequency along the lattice direction. They are hardly visible in optimal operation but can be enhanced by applying long pulses of 200 ms duration at the maximum available power (2 mW) of the probe beam. The resulting spectrum is plotted in grey in Fig. 2. The 1:5 ratio between the red and blue sidebands show that 80% of the atoms populate the $|n_z = 0\rangle$ motional state along the lattice axis, corresponding to a temperature of 8 μK. The transverse temperature is 10 μK.

The effect of the trap on the clock transition is measured by locking the frequency of the probe laser to the carrier for various values of U_0 and λ_L. The trap depth U_0 is adjusted to its desired value between $200\,E_r$ and $1400\,E_r$ by a linear ramp of 1 ms duration between the cooling and probing phases. This slightly decreases the transverse temperature while the longitudinal motion is adiabatically cooled by following the ramp. To lock the probe laser frequency we alternatively probe both sides of the resonance and compute an error signal from the difference between two successive measurements of the transition probability. This also gives a measurement of the difference between the atomic transition and the reference cavity frequency which slowly fluctuates due to thermal effects. These fluctuations behave essentially as a sine wave of peak to peak amplitude 300 Hz and period 10 minutes. To derive the frequency shift due to the lattice, we reject the cavity frequency fluctuations by a factor 100 by a differential method [15]. We interleave measurements at 4 different lattice depths. We run the

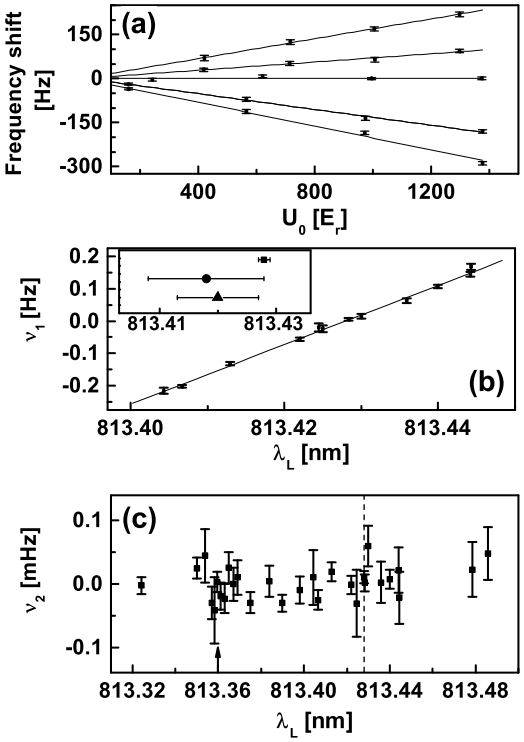

FIG. 3: (a): Frequency shift of the clock transition vs lattice depth for 5 different lattice wavelength: 813.406 nm (four lowest points in the graph), 813.413 nm, 813.428 nm, 813.436 nm and 813.444 nm (four highest points). Also shown is a linear fit of each of these five sets of data. (b): First order frequency shift vs λ_L for $U_0 = E_r$. Also plotted is a linear fit of these data ($\chi^2 = 1.1$). The inset shows measurements of λ_m. ■ : this work. ▲ : Ref. [2]. ● : Ref. [3]. (c): Higher order frequency shift vs λ_L for $U_0 = E_r$. All these points are compatible with zero. Their average is $-4(36) \times 10^{-7}$ Hz ($\chi^2 = 1.02$). The arrow on the λ_L axis corresponds to the $^3P_0 \rightarrow {}^1P_1$ transition at 813.360 nm. The vertical dotted line is at the magic wavelength 813.428 nm.

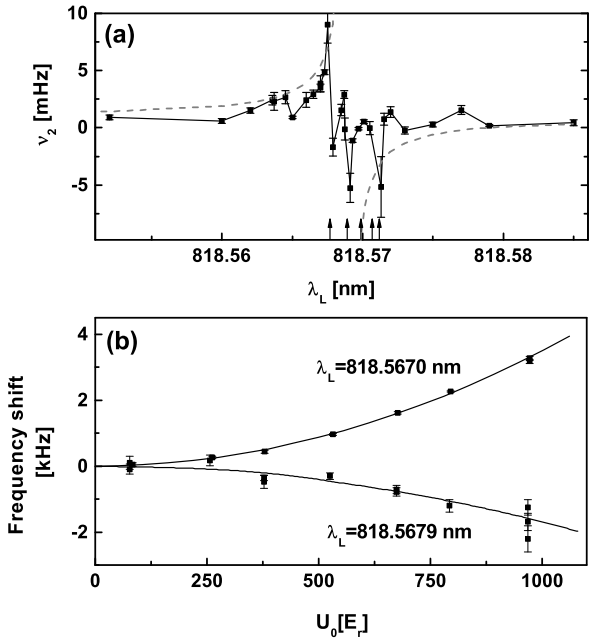

FIG. 4: (a): Higher order frequency shift around the $^3P_0 \rightarrow {}^3F_2$ transition at 818.570 nm for $U_0 = E_r$. The five vertical arrows on the wavelength axis correspond to the hyperfine sub-states of $5s4f\,{}^3F_2$ ($F = 13/2$ to $F = 5/2$ from left to right). (b): Atomic frequency shift vs trapping depth for two lattice wavelengths on both sides of the two-photon transition to sub-state $F = 13/2$. The linear light shift has been removed for clarity. The bold line is a fit of the data with a parabola.

clock for 19 cycles before U_0 is changed to the next of the four interleaved values. The entire sequence is repeated typically 16 times. The cavity fluctuations are then modelled as a polynomial which is determined by a least square fit of the data [18]. The data are corrected for the modelled cavity frequency fluctuations and averaged. This yields 4 statistically independent measurements [19] of the clock transition frequency versus U_0 with a standard deviation of about 5 Hz. A typical set of such points is shown in Fig. 3(a).

We perform a quadratic least square fit of each set of four points which gives a measurement of the coefficients ν_1 and ν_2 of Eq.(1). The coefficient ν_2 is plotted in Fig. 3(c) and found compatible with zero for the whole range [813.3 nm, 813.5 nm] to within a few tens of μHz. A specially interesting wavelength region is around 813.36 nm where the $^3P_0 \rightarrow {}^1P_1$ two-photon transition is expected. The contribution of a two-photon transition to ν_2 varies as Δ^{-1}, with Δ the detuning of the lattice with respect to the resonance. We magnify this contribution by systematically spanning a frequency range of ± 5 GHz with a 1 GHz step around the expected value (Fig. 3(c)). The null results of all these measurements demonstrate that the higher order shift due to the $^3P_0 \rightarrow {}^1P_1$ transition is less than $1\,\mu\text{Hz}/E_r^2$ for $\lambda_L = \lambda_m$. Despite its proximity to the magic wavelength, this two-photon transition is forbidden enough to not be a problem.

This set of experiments around 813.4 nm can also be used to derive an accurate value of λ_m. Having shown that ν_2 is negligible for $\lambda_L \sim \lambda_m$, better estimates of ν_1 are obtained with linear fits of each set of four points. They are plotted in Fig. 3(b). We find $\lambda_m = 813.428(1)$ nm in agreement with previously published values [2, 3] as shown in the inset of Fig. 3(b). The improvement by one order of the accuracy of this measurement is a nice illustration of the amplification of the effects of the lattice offered by a deep trapping potential.

We also studied the effect of the other two photon transition in this wavelength region, the $^3P_0 \rightarrow {}^3F_2$ at 818.57 nm. When tuned 5 nm away from λ_m we expect, in addition to the effect of the two-photon coupling, a trivial

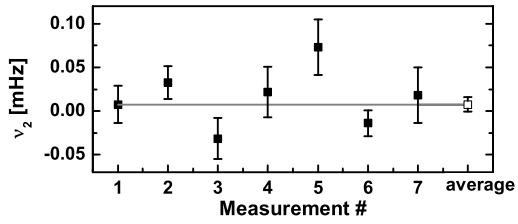

FIG. 5: Higher order frequency shift at the magic wavelength for $U_0 = E_r$. The value of the open square is the weighted average of the seven other points ($\chi^2 = 1.8$).

quadratic dependence of the atomic frequency vs U_0 due to the imperfect cancellation of ν_1 and to the inhomogeneity of the laser intensity experienced by the atoms. We do observe a substantial broadening and asymmetry of the resonance due to this effect similar to what was reported in Ref. [16]. The associated trivial quadratic frequency shift amounts to $0.8\,\mathrm{mHz}/E_r^2$ as measured several GHz away on both sides of the two photon transition.

When tuned closer to the resonance, we clearly observe the non-trivial quadratic frequency shift due to the two-photon resonance itself. The effect is shown in Fig. 4. Quadratic frequency shifts of several kHz and changing sign depending on the side of the transition being probed are observed as shown in Fig. 4(b). This is a clear signature of the higher order effects due to the particular transition under investigation. When tuned exactly onto one of the five transitions corresponding to the hyperfine structure of $^3F_2$, the lattice laser induces severe loss (up to 90%) of atoms when the 698 nm probe laser is tuned to resonance. This effect, which we attribute to three-photon ionization from $^3P_0$, was used to determine the position of the five hyperfine sub-states shown by arrows in Fig. 4(a). The hyperfine structure of $^3F_2$ leads to a complex dependence of the quadratic frequency shift on the lattice wavelength around resonance. The contribution of the five substates can interfere with each other, which may be the cause of the oscillations of ν_2 seen in Fig. 4(a) on both sides of the hyperfine manifold. We can deduce from our measurements a conservative estimate of the contribution of the $^3P_0 - {}^3F_2$ resonance to the higher order effects at $\lambda_L = \lambda_m$. The grey dashed curved plotted in Fig. 4(a) scales as the inverse of the detuning of the lattice with respect to the center of gravity of the hyperfine structure of $^3F_2$ and envelopes experimental points. When extrapolated to the magic wavelength, it gives a contribution to ν_2 of $2\,\mu$Hz.

Finally we have performed an extensive series of measurements of ν_2 at $\lambda_L = \lambda_m$ resulting in the data plotted in Fig. 5. Their weighted average gives $\nu_2(\lambda_m) = 7(6)\,\mu$Hz. For a lattice depth of $10\,E_r$ the frequency shift is lower than 1 mHz (one sigma) or 2×10^{-18} in fractional units. This demonstrates that the frequency shift due to the atomic hyperpolarizability constitutes no impediment to the accuracy of a Sr optical lattice clock down to the 10^{-18} level. In addition, the effective laser intensity seen by the atoms is certainly controllable at the percent level [20]. The performance of the system would then be immune to higher order frequency shifts over a broad lattice depth range, possibly up to $U_0 = 100\,E_r$. This would provide a powerful lever for the experimental evaluation at the 10^{-18} level of other effects associated for instance to the dynamics of the atoms in the lattice or to cold collisions. Collisions are expected negligible with polarized fermions, but they have to be considered if one uses bosonic isotopes [4], such as ^{88}Sr. By varying the trapping depth, one can adjust the tunnelling rate and then control the overlap of the wave functions of atoms confined in the lattice, allowing the study of cold collisions in a new regime.

We thank A. Clairon and C. Salomon for useful comments and discussions on the manuscript. SYRTE is Unité Associée au CNRS (UMR 8630) and a member of IFRAF (Institut Francilien de Recherche sur les Atomes Froids). This work is supported by CNES.

* Electronic address: pierre.lemonde@obspm.fr

[1] H. Katori, M. Takamoto, V. G. Pal'chikov, and V. D. Ovsiannikov, Phys. Rev. Lett. **91**, 173005 (2003).
[2] M. Takamoto, F.-L. Hong, R. Higashi, and H. Katori, Nature **435**, 321 (2005).
[3] A. D. Ludlow *et al.*, ArXiv:physics/0508041 (2005).
[4] Z. W. Barber *et al.*, arXiv:physics/0512084 (2005).
[5] U. Sterr *et al.*, C. R. Physique **5**, 845 (2004).
[6] H. S. Margolis *et al.*, Science **306**, 1355 (2004).
[7] W. H. Oskay, W. M. Itano, and J. C. Bergquist, Phys. Rev. Lett. **94**, 163001 (2005).
[8] T. Schneider, E. Peik, and C. Tamm, Phys. Rev. Lett. **94**, 230801 (2005).
[9] P. Dubé *et al.*, Phys. Rev. Lett. **95**, 033001 (2005).
[10] P. Lemonde and P. Wolf, Phys. Rev. A **72**, 033409 (2005).
[11] G. Grynberg and B. Cagnac, Rep. Prog. Phys. **40**, 791 (1977).
[12] I. Courtillot *et al.*, Opt. Lett. **28**, 468 (2003).
[13] T. Mukaiyama *et al.*, Phys. Rev. Lett. **90**, 113002 (2003).
[14] A. Quessada *et al.*, J. Opt. B **5**, S150 (2003).
[15] Y. Sortais *et al.*, Phys. Rev. Lett. **85**, 3117 (2000).
[16] M. Takamoto and H. Katori, Phys. Rev. Lett. **91**, 223001 (2003).
[17] All wavelengths throughout the paper are in vacuum.
[18] We use a tenth order polynomial fit of the data. For any polynomial order between 5 and 14, the results are unchanged to within a fraction of the error bars.
[19] except for a common offset which doesn't play any role in further data analysis.
[20] A control to within a few percents is already achieved in our setup as evidenced by the nice alignement of the measurements of ν_1 shown in Fig. 3(b).